



American Society of Hematology
2021 L Street NW, Suite 900,
Washington, DC 20036
Phone: 202-776-0544 | Fax 202-776-0545
editorial@hematology.org

Azithromycin promotes relapse by disrupting immune and metabolic networks after allogeneic stem cell transplantation

Tracking no: BLD-2022-016926R1

Nicolas Vallet (INSERM U976, France) Sophie Le Grand (INSERM U976, France) Louise Bondeelle (Pneumology unit, Saint Louis Hospital, Assistance Publique-Hopitaux de Paris, France) Benedictine Hoareau (UPMC, France) Aurelien Corneau (Sorbonne Université, INSERM UMS037 PASS, Plateforme de Cytométrie (CyPS), France) Delphine Bouteiller (Genotyping and Sequencing Facility, Paris Brain Institute - ICM, France) Simon Tournier (Core Facilities, Saint Louis Research Institute, Université de Paris Cité, UAR 2030 / US 53, France) Lucille Derivry (INSERM U976, France) Armelle Bohineust (INSERM U976, France) Marie Tourret (Institut national de recherche médicale (INSERM) UMR976, Université de Paris, Paris, France, France) Delphine Gibert (INSERM U976, France) Ethan Mayeur (INSERM U976, France) Raphaël Itzykson (Hopital Saint-Louis, France) Kim Pacchiardi (INSERM U944, France) Brian Ingram (Metabolon Inc., United States) Stephane Cassonnet (Service de Biostatistique et Information Médicale, France) Patricia Lepage (Micalis Institute, INRA, AgroParisTech, Paris-Saclay University, Jouy-en-Josas, France, France) Régis Peffault de Latour (Saint-Louis, France) Gérard Socie (Hematology Transplantation, France) Anne Bergeron (Pneumology Department, Geneva University Hospitals, Switzerland) David Michonneau (Université de Paris Cité, INSERM U976, France)

Abstract:

Administration of azithromycin after allogeneic hematopoietic stem cell transplantation for hematological malignancies has been associated with relapse in a randomized phase 3 controlled clinical trial. Studying 240 samples from patients randomized in this trial is a unique opportunity to better understand the mechanisms underlying relapse, the first cause of mortality after transplantation. We used multi-omics on patients' samples to decipher immune alterations associated with azithromycin intake and post-transplant relapsed malignancies. Azithromycin was associated with a network of altered energy metabolism pathways and immune subsets, including T cells biased toward immunomodulatory and exhausted profiles. In vitro, azithromycin exposure inhibited T cells cytotoxicity against tumor cells and impaired T cells metabolism through glycolysis inhibition, mitochondrial genes downregulation, and immunomodulatory genes upregulation, notably SOCS1. These results highlight that azithromycin directly affects immune cells that favor relapse, which raises caution about long-term use of azithromycin treatment in patients at high risk of malignancies.

Conflict of interest: COI declared - see note

COI notes: G.S. and R.P.L received a research grant from Alexion Pharmaceutical Company. R.P.L received a research grant from Novartis and Pfizer companies. G.S received fees from Pharmacyclics LLC, Novartis, Incyte, Alexion, Amgen and Pfizer companies. D.M received fees from Novartis, Incyte, Jazz Pharmaceuticals and CSL Behring companies. All other authors have no conflict of interests to declare.

Preprint server: No;

Author contributions and disclosures: Conceptualization: AB, DM; Methodology: DM, NV; Formal analysis: NV, SLG; Figures generation: NV, SLG, DM; Investigation: NV, SLG, LB, AC, BH, DB, LD, AB, MT, DG, EM, RI, KP, BI, PL; Resource: NV, AC, ST, PL, RPL, DM; Data Curation: NV, LB; Writing - Original Draft: NV, DM; Writing - Review and Editing: GS, AB, DM; Visualization: NV, DM; Supervision: DM; Project Administration: AB, DM; Funding Acquisition: GS, AB, DM

Non-author contributions and disclosures: No;

Agreement to Share Publication-Related Data and Data Sharing Statement: Raw data are available on public repository: (i) mass cytometry: FlowRepository FR-FCM-Z5ZB and FR-FCM-Z5L7; (iii) metabolomic: Metabolights MTBLS406; (iv) single-cell RNA sequencing: GEO GSE197658 and GSE208399. Analysis pipeline are available on Git repositories: <https://gitlab.com/nivall/azimut-blood>; <https://gitlab.com/nivall/azimut-in-vitro>; <https://gitlab.com/nivall/azimutscrna>

Clinical trial registration information (if any):

Title: Azithromycin promotes relapse by disrupting immune and metabolic networks after allogeneic stem cell transplantation

Short title: Azithromycin inhibits anti-tumor immune response

Authors: Nicolas Vallet¹, Sophie Le Grand¹, Louise Bondeelle², Bénédicte Hoareau³, Aurélien Corneau³, Delphine Bouteiller⁴, Simon Tournier⁵, Lucille Derivry¹, Armelle Bohineust¹, Marie Tourret¹, Delphine Gibert¹, Ethan Mayeur¹, Raphael Itzykson⁶, Kim Pacchiardi⁶, Brian Ingram⁷, Stéphane Cassonnet^{2,8}, Patricia Lepage⁹, Régis Peffault de Latour^{10,11}, Gérard Socié^{1,10†}, Anne Bergeron^{12†}, David Michonneau^{1,10*}

Affiliations:

¹Université de Paris Cité, INSERM U976; F-75010, Paris, France.

²Pneumology unit, Saint Louis Hospital, Assistance Publique-Hopitaux de Paris; Paris, France.

³Plateforme de Cytométrie de la Pitié-Salpêtrière (CyPS), UMS037-PASS, Sorbonne Université - Faculté de Médecine; F-75013, Paris, France.

⁴Genotyping and Sequencing Facility, Paris Brain Institute - ICM, Hôpital de la Pitié-Salpêtrière, CNRS UMR 7225, Inserm U1127, Sorbonne Université UM75, CS21414 75646; Paris, France.

⁵Core Facilities, Saint Louis Research Institute, Université de Paris Cité, UAR 2030 / US 53; 75010, Paris, France.

⁶INSERM UMR 944, IRSL, St Louis Hospital, University of Paris Cité; Paris, France.

⁷Metabolon, Inc.; Morrisville, North Carolina, 27560, USA.

⁸Service de Biostatistique et Information Médicale, Hôpital Saint-Louis, AP-HP; Paris, France.

⁹Université Paris-Saclay, INRAE, AgroParisTech, Micalis Institute; Domaine de Vilvert, 78350, Jouy-en-Josas, France.

¹⁰Hematology Transplantation, Saint Louis Hospital; 1 avenue Claude Vellefaux, 75010 Paris, France.

¹¹Cryostem Consortium.

¹²Pneumology Department, Geneva University Hospitals; Geneva, Switzerland.

†These authors contributed equally to this work.

***Corresponding author**

David Michonneau

Hematology and transplantation unit

Saint Louis hospital

1 avenue Claude Vellefaux

75010 Paris, France

Phone 33 1 71 20 75 90

Fax 33 1 42 49 96 36

Email: david.michonneau@aphp.fr

Word counts: 4000

Abstract word counts: 149

Figure number: 7

Table number: 0

References: 49

Scientific category: transplantation

Key points (50 words):

- Azithromycin after allogeneic hematopoietic stem cell transplantation increases relapse of malignancies in a randomized-placebo trial.
- Azithromycin dampens anti-tumor immune response by disrupting T cell functions through inhibition of energy metabolism in immune cells.

Abstract (149 words): Administration of azithromycin after allogeneic hematopoietic stem cell transplantation for hematological malignancies has been associated with relapse in a randomized phase 3 controlled clinical trial. Studying 240 samples from patients randomized in this trial is a unique opportunity to better understand the mechanisms underlying relapse, the first cause of mortality after transplantation. We used multi-omics on patients' samples to decipher immune alterations associated with azithromycin intake and post-transplant relapsed malignancies. Azithromycin was associated with a network of altered energy metabolism pathways and immune subsets, including T cells biased toward immunomodulatory and exhausted profiles. In vitro, azithromycin exposure inhibited T cells cytotoxicity against tumor cells and impaired T cells metabolism through glycolysis inhibition, mitochondrial genes downregulation, and immunomodulatory genes upregulation, notably SOCS1. These results highlight that azithromycin directly affects immune cells that favor relapse, which raises caution about long-term use of azithromycin treatment in patients at high risk of malignancies.

INTRODUCTION

Allogeneic hematopoietic stem cell transplantation (allo-HSCT) is a curative treatment for hematologic malignancies. Significant efforts aim to improve the survival and quality of life of patients suffering from acute or chronic graft-versus-host-disease (GvHD)¹⁻⁴. Lung chronic GvHD, including bronchiolitis obliterans syndrome (BOS), affects about 10% of patients and is associated with poor outcomes⁵⁻⁷. Azithromycin was shown to prevent BOS following lung transplantation⁸. These observations led us to investigate if azithromycin could prevent BOS in a multicenter, randomized, placebo-controlled, double-blind, phase 3 study (ALLOZITHRO trial). Unexpectedly, azithromycin did not efficiently prevent BOS, and was associated with higher mortality due to an increased risk of relapse (hazard ratio [HR]=1.7, p=0.002). This led to an early interruption of the study⁹ and both a Food and Drug Administration and European Medicines Agency warnings about azithromycin use after allo-HSCT¹⁰. In a multicenter retrospective setting, azithromycin treatment for BOS after HSCT was also associated with a higher risk of secondary neoplasms¹¹.

Anti-tumoral effects of allo-HSCT rely on immune-mediated mechanisms by donor cells¹² and relapse is the first cause of death following allo-HSCT¹³. Relapse involves immune escape mechanisms including downregulation of class II major histocompatibility complex (MHC) and expression of co-inhibitory molecules¹⁴⁻¹⁶. T cells are indeed associated with higher expression of co-inhibitory molecules, exhausted cells subsets, and defective effector functions^{15,17}. Likewise, in autologous chimeric antigen receptor (CAR)-T cells infusions, T cells exhaustion is associated with a lower response rate¹⁸.

Analyzing biological samples of patients from the ALLOZITHRO trial is a unique opportunity to decipher immune alterations associated with azithromycin and relapse after allo-

HSCT. We applied mass cytometry and non-targeted metabolomics, to determine the impact of azithromycin on immune subsets and the metabolome of patients. This approach revealed that azithromycin treatment altered the frequency of many immune subsets together with alteration of their functional states. Considering that azithromycin could alter host or bacteria metabolism, we then examined the plasma and cellular metabolomes^{19,20}. Integration of biological variables associated with azithromycin intake and clinical data highlighted an immuno-metabolic network associated with tumor relapse after allo-HSCT. We next uncovered the inhibitory properties of azithromycin on major T cells functions, including proliferation, cytokines production, cytotoxicity against leukemic targets. Finally, we studied how azithromycin impairs T cells metabolism during activation through glycolysis inhibition, downregulation of mitochondrial and pro-inflammatory gene expression, and upregulation of immune suppressive genes.

METHODS

Study design

This study was conducted with samples from patients included in the ALLOZITHRO trial (NCT01959100)⁹ and approved by the local ethic committee and Institutional Review Board (CPP Ile de France IV, IRB number 00003835, reference number 2013-000499-14). Samples were retrieved from CRYOSTEM Consortium²¹ (project number CS-1801, validated by IRB Sud-Méditerranée 1, reference number AC-2011-1420) and the Commission National Informatique et Liberté for data protection (reference number nz70243374i n°912120). All patients gave their written consent for clinical research. This non-interventional research study was carried out in accordance with the Declaration of Helsinki. Data analyses were performed using databases without patient identifiers. Healthy donor PBMC were isolated from residual blood after apheresis provided by *Etablissement Français du Sang* (18/EFS/032).

Experimental procedures

Details on experimental assays are described in **Supplemental Methods**.

Data and code sharing: Raw data are available on public repository: (i) mass cytometry: FlowRepository FR-FCM-Z5ZB and FR-FCM-Z5L7; (iii) metabolomic: Metabolights MTBLS406; (iv) single-cell RNA sequencing: GEO GSE197658 and GSE208399. Analysis pipeline are available on Git repositories: <https://gitlab.com/nivall/azimut-blood>; <https://gitlab.com/nivall/azimut-in-vitro>; <https://gitlab.com/nivall/azimutscrna>

RESULTS

Cohort description

Samples from azithromycin (n=123) and placebo (n=117) patients were collected at a median time of 85 and 84 days after allo-HSCT, respectively (**Figure 1**)²¹. Characteristics of patients' subsets within omics cohorts were comparable between azithromycin and placebo groups (**Table S1**). There was no major disparity in co-medication received by both groups, and azithromycin levels in metabolomic was not influenced by other drugs (**Supplemental methods**). Consistent with the findings of the ALLOZITHRO trial, a higher risk of relapse with azithromycin was observed in patients studied herein (**Supplemental Figure S1**).

Patients treated with azithromycin exhibit reduced circulating T cells and higher anti-inflammatory subsets

We first ruled out that azithromycin could increase tumor cell proliferation or survival. Fourteen AML cell lines and primary leukemic cells from 8 patients were cultured with azithromycin. Regardless of azithromycin concentration, azithromycin was not associated with an effect on cell expansion (**Supplemental Figure S2 and S3**).

We then focused on circulating immune cells in patients' samples. To identify main PBMC cell subsets, FlowSOM algorithm²² was performed on CD45⁺ living cells using 31 phenotypical markers (**Figure 2A**). Antigen expressions in the 55 phenotypical clusters were then manually checked to identify the corresponding cells subsets (**Figure 2B-C, Supplemental Figure S4, Table S2**). We found that patients included in the azithromycin arm were associated with a lower abundance of T cells (p=0.024), while no difference was observed for B, NK, or

myeloid lineage (**Figure 2D**). Next, we compared the frequency of phenotypical clusters among these subsets. Azithromycin-treated patients were characterized by higher central memory (CM) and effector memory (EM) CD4⁺ T cells with a Th2 profile defined by CXCR3⁻CCR4⁺ ($p=0.045$ and $p=0.010$, respectively). A higher frequency of CCR5⁻FoxP3^{lo} regulatory T cells (Tregs) was also found in azithromycin-treated patients ($p=0.003$). Azithromycin treatment was associated with a higher frequency of activated CM CD8⁺ cells characterized by high HLA-DR, CD38, and PD-1 expression, suggesting an exhausted phenotype ($p=0.033$). Finally, azithromycin intake was associated with lower switched memory CD5⁻CXCR3⁻CCR7⁺ B cells ($p=0.033$), with a higher abundance of immature CD56^{hi}CCR5^{lo} NK cells ($p=0.003$) and lower frequency of cluster 40 among unidentified cells ($p=0.016$) (**Figure 2E-F, Supplemental Figure S5-S6**).

Azithromycin intake is associated with exhausted T cells phenotypes

We then studied T cell functional profiles with 14 additional functional markers using the FlowSOM algorithm. We identified 25 clusters representing activation or functional states of cells (**Figure 3A**). Three main profiles emerged: (i) activated cells characterized by the expression of granzyme B, Eomes or T-bet; (ii) naïve cells characterized by low levels of expression of most functional markers; and (iii) exhausted cells characterized by higher levels of TOX, PD-1, ICOS, CTLA-4, 4-1BB, LAG-3 and TIM-3 (**Figure 3A**).

We next compared abundances of functional clusters among phenotypical clusters in azithromycin and placebo patients. We identified four T cells subsets significantly increased in azithromycin patients: TIGIT⁺ (functional state 16) in regulatory T cell CCR5⁻FOXP3^{lo} (cluster 3) ($p=0.033$) and in CM Th2 CD4⁺ PD1⁻CD25⁺ (cluster 2) ($p=0.034$), KLRG1⁺2B4⁺TIGIT⁺ (functional state 8) in CM CD8⁺PD1⁺CD38⁻ (cluster 28) ($p=0.048$) and

TIGIT⁺KLRG1⁺2B4^{lo}PD-1^{lo}TOX^{lo}Eomes⁺ (functional state 6) in CM double negative subset (cluster 21) ($p=0.029$). Activated cytotoxic GranzymeB⁺PD-1^{lo} (functional state 10) in CM CD8⁺PD-1⁺CD38⁺ cell (cluster 36) was found to be decreased in azithromycin patients ($p=0.039$) (**Figure 3A-B**).

Together these results highlight that, patients treated with azithromycin were characterized by lower T cells abundance and were biased toward immunomodulatory Th2 response, with increased FoxP3⁺ regulatory T cells and exhausted phenotypes characterized by the expression of TOX, PD-1, and TIGIT.

Azithromycin is associated with variations in cell energy metabolism metabolites

We then explored if azithromycin intake could impact plasma metabolome, considering that azithromycin could alter host- or microbiota-related metabolism^{19,23}. We studied metabolites from frozen plasma and dried white blood cells pellets to uncover both circulating and intracellular metabolomic profiles. 853 and 352 metabolites were studied in plasma and dried cell pellets, respectively (**Supplemental Figure S7**).

In plasma, 73 metabolites were significantly different between patients who received azithromycin and those from the placebo group. The most statistically significant changes were observed for (i) imidazole propionate, a microbial histidine-derived metabolite and precursor of glutamate²⁴, lowered in the azithromycin group and (ii) plasmalogen metabolites with higher levels in azithromycin than placebo (**Figure 4A, Supplemental Table S3**). Imidazole propionate is a key regulator of glucose metabolism and an activator of the mTOR pathway²⁴. Enrichment analysis of the significant metabolites revealed an overrepresentation of plasmalogen and acyl-carnitine (polyunsaturated) pathways. Oxidative phosphorylation (OXPHOS), pantothenate, and

purine metabolism pathways were the most enriched but not statistically significant (**Figure 4A**, **Supplemental Table S4**).

We then explored the intracellular metabolome and identified 10 significantly different metabolites between the two groups (**Figure 4B**, **Supplemental Table S5**). Heptanoate was the most significantly lowered metabolite in the azithromycin group. This metabolite is a medium-chain fatty acid (MC-FA) involved in the tricarboxylic acid cycle (TCA) by acetyl-coenzyme A (CoA) and succinyl-CoA biosynthesis through mitochondrial beta-oxidation of long-chain fatty acid²⁵. The MC-FA pathway was significantly enriched (**Figure 4B**, **Supplemental Table S6**).

Altogether these results underline changes in pathways converging to acetyl-CoA synthesis from mitochondrial beta-oxidation through enrichment in acyl-carnitine and MC-FA pathways for its use in OXPHOS. CoA was recently found to enhance CD8⁺ Tc22 anti-tumoral functions²⁶. Here, the precursor of CoA, pantothenate, was increased in the azithromycin group. This may be related to the metabolite accumulation because of lower incorporation in CoA as reported when inhibiting pantothenate kinase (PANK)²⁷. Supporting this hypothesis, acyl-carnitine metabolites were higher in azithromycin patients as observed within PANK inhibited hepatocytes (**Supplemental Table S3**)²⁷. Additionally, the enrichment in plasmalogens suggests that immune-regulatory pathways are involved in the azithromycin effect as higher levels of plasmalogens are associated with post-transplant immune tolerance²⁸.

Variables associated with azithromycin intake are also associated with relapse

To study the interactions between variables significantly associated with treatment groups and determine whether these variables were also associated with relapse, we studied patients with malignancies for which we had all biological data (multi-omics cohort) (**Figure 1**,

Supplemental Table S1). In these patients, sample collection preceded relapse at a median time of 6.36 (interquartile range [IQR]: 1.92-12.03) months in the azithromycin group and 16.58 (IQR: 5.14-25.05) months in the placebo group, and azithromycin intake was associated with a higher cumulative incidence of relapse (HR=1.81, 95%CI [1.10-3.02], p=0.02). We first determined if differences associated with azithromycin intake were more pronounced in patients who relapsed (**Supplemental Figure S8**). Immune subsets and metabolites whose variations were associated with azithromycin intake were also analyzed individually for their association with relapse (**Supplemental Table S7**).

Since these variables may be associated with relapse in a multivariate manner, we used principal component analysis to perform dimension reduction (**Figure 4C, Supplemental Figure S9A**). Then, to measure the association of these components with relapse, we used a multivariate competing Fine and Gray risk model that included treatment groups as covariate. Three components (#7, #13, #25) were significantly associated with relapse (**Figure 4D, Supplemental Table S8**), and all omics layers contributed to these components (**Figure 4E**).

Variables that contributed to at least 1% of components were considered as significant contributors and thus were associated with relapse (**Supplemental Figure S9B-D**). Among the 94 variables that differed between azithromycin and placebo patients, 59 contributed significantly. Cell subsets were PD1⁺ CM CD4⁺ Th2 (cluster 4), CD56^{hi}CCR5^{lo} NK cells (cluster 38) and switched memory B cells (cluster 34), CM CD8+ T cells PD1+CD38+ (cluster 36), TIGIT⁺ (state 16) in PD1⁻ CM Th2 (cluster 2), KLRG1+2B4+TIGIT+ (state 8) in CM CD8+ PD1+CD38- (cluster 28) and Granzyme B⁺ and PD1^{lo} (state 10) in CM CD8+ (cluster 36). Interestingly, one of the first contributors was white blood cells intracellular 2,3-diphosphoglycerate, a metabolite involved in glycolysis. Enriched plasmatic pathways included

(i) energy metabolism: Fatty Acid Dicarboxylate, CoA Metabolism, (ii) immunomodulator mechanisms: pregnenolone steroids, primary bile acid, plasmalogen and (iii) purine and pyrimidine metabolism (**Supplemental Figure S10A**). In cells, most enriched metabolomic pathways also encompassed energy metabolism: MC-FA, and dinucleotides (**Supplemental Figure S10B**).

To highlight inter-omics relationships, we next performed correlations analyses. The distribution of significant correlations across omics and variables correlations are depicted in **Figure 4F-G**. The correlation network identified different clusters of variables in which at least one variable contributed to relapse. State 8 ($\text{TIGIT}^+ \text{KLRG1}^+ \text{2B4}^+$) in CM CD8 $^+$ PD1 $^+$ CD38 $^-$ (cluster 28) were correlated with 3-Carboxy-4-methyl-5-propyl-2-furanpropionic acid (3-CMPF), a uremic toxin known to inhibit mitochondrial respiration (**Figure 4G**).

Altogether these results illustrate that among variables associated with azithromycin intake, Th2 and exhausted T cells, and energy metabolism pathways, notably glycolysis-derived metabolites, contributed specifically to relapse.

Azithromycin intake is associated with transcriptional changes in energy metabolism, cell cycle and inflammation pathways

We then performed single-cell RNA sequencing coupled with cellular indexing of epitopes (CITE-seq) on 31 patients' samples (**Figure 5A and Table S9**). Clustering 65,382 cells using cell surface antigen expression allowed the identification of 23 immune subsets (**Figure 5B-C**).

Gene set enrichment score was calculated in each subset after differential gene expression analyses. Consistent with our metabolomic results, metabolism pathways were enriched in immune cells, including OXPHOS, glycolysis, cholesterol and fatty acid metabolism. Immune

functions were also influenced by azithromycin exposure, including IFN- α and IFN- γ responses, complement pathway, inflammatory response and cytokine signaling pathways. Signaling pathways involved in immune response such as mTORC1, STAT3, STAT5 and NFkB signaling pathways were enriched. Finally, cell cycle related pathways (E2F, mitotic spindle, G2M checkpoint, MYC) were enriched in various cell subsets (Figure 5D). Since T cells frequency was lowered in azithromycin patients, we calculated cell cycle score in T cells main subsets. We found that higher frequency of CD4 $^{+}$ T cells were in G2M phases ($p=0.032$) (**Figure 5E**).

Azithromycin exposure does not affect class II MHC expression by antigen presenting cell or tumor cell

Downregulation of class II HLA has been previously involved in post-transplant relapses¹⁴. Azithromycin was not associated with downregulation of HLA-DR expression on antigen presenting cells (APC) from ALLOZITHRO trial samples. Transcriptomic assays did not unveil a downregulation of class II gene expression. *In vitro*, APC exposed to azithromycin did not lower HLA-DR DQ DP proteins expression. Primary leukemic cells exposed to azithromycin were not associated with lower expression of HLA-DR DQ DP proteins (**Supplemental Figure S11**).

Azithromycin modulates T cells functions by inhibiting glycolysis during activation

To evaluate if azithromycin may have a direct impact on PBMCs and since azithromycin was associated with a lower abundance of T cells and higher frequency of G2M CD4 $^{+}$ T cells, we studied the effects of azithromycin on T cells proliferative functions *in vitro*. CD3 $^{+}$ -sorted cells from HD were incubated for 24 hours with azithromycin at 10 mg.L $^{-1}$ and 20 mg.L $^{-1}$ before

activation with anti-CD3/CD28 beads to mimic the azithromycin intake before allo-HSCT. After 48 hours of culture, we observed a dose-dependent inhibition of CD4⁺ and CD8⁺ T cells proliferation (**Figure 6A**). Cell viability was not impacted by azithromycin (**Supplemental Figure S12A-B**). The effect of azithromycin on proliferation was reversible after a wash-out of 24 hours before activation (**Supplemental Figure S13**). This result confirms a specific effect of azithromycin on T cells and is not in favor of a non-specific toxic effect.

We then treated the cells with cyclosporin A to mimic the effect of GVHD prophylaxis. This revealed that effects of azithromycin and cyclosporin A were additive in CD8⁺ T cells and that azithromycin at 10 mg.L⁻¹ had an inhibitory effect comparable to cyclosporin at a usual dose of 150 ng.mL⁻¹ (**Supplemental Figure S14**).

Next, to assess if azithromycin might also affect cytokine production functions, we studied cytokines levels on T cells supernatant with multiplex immunoassays. After two days of activation, all evaluated cytokines except IL-4 and IL-13 were dose-dependently reduced in supernatants from azithromycin-treated cells. After five days of activation, IL-13 levels were increased by azithromycin exposure (**Supplemental Figure S15-S17**). These results revealed that azithromycin inhibited the secretion of pro-inflammatory and anti-tumoral cytokines such as IL-2, IL-15, IL17, IFN- γ , IFN- α and TRAIL. Consistent with a higher abundance of Th2 subsets in patients from the clinical trial, azithromycin promoted the Th2 pathway *in vitro*, as illustrated by a higher IL-13 level.

To unravel whether azithromycin could inhibit anti-tumoral T cells cytotoxic functions, anti-CD19 chimeric antigen receptor (CAR)-T cells were cultured for 24 hours with azithromycin then incubated with CD19⁺ NALM6 lymphoblastic leukemia cells line. The

percentage of specific lysis was dose-dependent and reduced by azithromycin (**Figure 6B**). Treatment did not impact CAR-T cells viability (**Supplemental Figure S12C**).

Metabolomic analyses revealed enrichment in energy metabolism pathways in azithromycin-treated patients and in relapsed patients. We thus hypothesized that azithromycin exposure could impair energy metabolism in T cells during the immune response. Since glycolysis plays a central role in ATP synthesis during T cells activation²⁹, we studied energy metabolism following anti-CD3/CD28 activation in T cells from HD. To characterize the impact of azithromycin on the CD3⁺ subtypes, CD4⁺ and CD8⁺ T cells were sorted and incubated for 24 hours in azithromycin 10 mg.L⁻¹. Glycolytic activity measured by extracellular acidification rate (ECAR) after T cell activation was reduced in CD4⁺ and CD8⁺ cells treated by azithromycin (**Figure 6C**). Mitochondrial oxidative phosphorylation measured by oxygen consumption rate (OCR) was not different between the two groups (**Figure 6C**). Our results argue that azithromycin dampens immune cell functions by inhibiting glycolysis during activation, while not affecting OXPHOS metabolism. This mechanism could impair normal T cells activation and differentiation during immune response after allo-HSCT.

Azithromycin inhibits TCR signaling pathways following activation

Using mass cytometry, we studied signaling pathways to evaluate if their inhibition may drive the dampening of glycolysis and effector functions. At five time-points following anti-CD3/CD28 activation we measured 14 signaling proteins among 23 PBMC subsets from eight HD (**Figure 7A and Supplemental Figures S18-S19**). Analysis disclosed an inhibition of TCR signaling in CD4⁺ Tregs and double negative subsets and in CM and EMRA CD8⁺ subsets.

Additional inhibition of pAkt, pmTOR, and pERK were also found in CD4⁺ subsets (**Figure 7B** and **Supplemental Figure S20**).

Azithromycin promotes immunomodulatory gene expression and disrupts mitochondrial mRNA synthesis

To explore whether azithromycin's impact on T cells was associated with phenotypical and transcriptional changes in CD4⁺ and CD8⁺ T cells, we perform CITE-seq on T cells from HD 48 hours following anti-CD3/CD28 activation. Cells were clustered according to cell surface antigen expression (**Figure 7C-D**). Cluster abundance did not differ between treated and untreated conditions (**Figure 7E**).

Transcriptomic analysis disclosed downregulation of pro-inflammatory genes: (i) *IFNG* in CD4+, in double-positive central memory (cluster 25) and Th1 (cluster 0) cells, and (ii) *MIF* in mostly all clusters (**Figure 7F** and **Supplemental Figure S21**). *SOCS1* was upregulated in most clusters (**Figure 7F**). Since SOCS1 was recently found to impair anti-tumor response in Th1 cells³⁰, we measured SOCS1 expression six days after activation by flow cytometry. We identified that SOCS1 expression was significantly higher in azithromycin-treated CD4⁺ (p=0.020) but not in CD8⁺ (p=0.074) T cells (**Supplemental Figure S22**).

Downregulation of genes implicated in ATP biosynthesis was also observed with azithromycin: (i) mitochondrial mRNA involved in the synthesis of mitochondrial complexes I (*MT-ND4*, *MT-ND5*), IV (*MT-CO3*) and V (*MT-ATP6*); (ii) *NAMPT*, involved in NAD synthesis, a required metabolite for mitochondrial complex I function (**Figure 7D**). Considering this impact of genes of the mitochondrial complex, we measured mitochondrial mass and function by flow cytometry. While we did not identify an impact of azithromycin on mitochondrial mass in CD4⁺ and CD8⁺, lower mitochondrial respiratory chain function was

identified with Tetramethylrhodamine, Methyl Ester, Perchlorate (TMRM) assays in CD4⁺ and CD8⁺ T cells (**Supplemental Figure S23**). Likewise, in resting T cells, basal and maximum mitochondrial respiration assed by OCR was reduced after 5 days of exposure to azithromycin *in vitro* (**Supplemental Figure S24**).

Altogether, these results show that azithromycin impairs lymphocyte effector functions through downregulation of mitochondrial complexes I, IV, and V genes and functions, and of genes with pro-inflammatory function while it upregulates SOCS1 expression, a negative regulator of the immune response.

DISCUSSION

Understanding mechanisms of relapse after allo-HSCT is mandatory to improve our comprehension of anti-tumor immune response and to develop new therapeutic approaches. Here, we took advantage of samples from patients included in a randomized study to decipher how azithromycin promoted relapse in patients. To gain mechanistic insight, we performed *in vitro* experiments which highlighted that azithromycin promotes immunomodulatory mechanisms, notably through inhibiting main anti-tumoral T cells functions.

We first identified immune changes associated with azithromycin intake in patients, including lower total T cells, a higher proportion of Th2-biased T cells, and an increased proportion of naïve FoxP3+ regulatory T cells. Functional states of immune cells revealed increased proportion of exhausted lymphocytes, notably expressing inhibitory receptors TIGIT and PD-1 with TOX³¹, associated with azithromycin treatment. Exhaustion mechanisms had been previously reported to be associated with relapse^{17,32,33}. Interestingly, similarly to what has been reported in non-responder to immune checkpoint inhibitors, we observed lower switched

memory B cells characterized by lower CXCR3 expression being associated with azithromycin intake³⁴.

To decipher azithromycin effects on anti-tumor response, we explored T cells functions after azithromycin exposure *in vitro*. It highlighted how azithromycin inhibits the proliferation of both CD4⁺ and CD8⁺ T cells after activation without impacting their survival. Azithromycin inhibited anti-tumor cytotoxicity functions of T cells and cytokine production, notably anti-tumor cytokines such as type 1 and 2 interferons and TRAIL³⁵⁻³⁷. In addition, higher level of IL-13, an interleukin that suppress type I responses in tumor environment³⁸, was consistent with Th2-biased cells subsets after azithromycin exposure.

By integrating biological variables associated with azithromycin intake, we identified the PD1⁺ Th2 CD4⁺, exhausted PD1⁺ CD8⁺ T cells and NK cells subsets as main contributors to subsequent relapse, as well as pathways involving energy metabolism and CoA biosynthesis. Imidazole propionate was lower in azithromycin patients. This histidine-derived metabolite activates mTOR-S6K pathway²⁷, and its absence in hepatocyte cultures is comparable to the effect of Rapamycin treatment, suggesting its importance in cell signaling²⁴. Coenzyme A has a central role in enhancing anti-tumor cytotoxicity by promoting oxidative phosphorylation in CD8⁺ T cells²⁶. In addition, 2,3-diphosphoglycerate involved in glycolysis was one of the first intracellular metabolite contributing to relapse. Metabolomic may be influenced by gut microbiota changes under azithromycin treatment or by changes in host metabolism that are not directly related to immune cells. Gene set enrichment from single cell transcriptomic analyses on PBMC from patients revealed that azithromycin was associated with enrichment in energy metabolism pathways like glycolysis, OXPHOS and fatty acid related pathways in immune cells. Direct effect on T cells metabolism was next confirmed *in vitro*, in which azithromycin exposure

inhibited glycolysis in both CD4⁺ and CD8⁺ subsets after activation. Glycolysis in T cells mobilizes ATP to gain effector functions following activation²⁹. Previous studies have demonstrated that glycolysis inhibition could induce T cell exhaustion^{39,40}. In addition, metabolically unfit T cells were found to be associated with lower anti-tumor activity⁴¹. Glycolysis is known to be regulated by the mTORC1-HIF1 pathway^{42,43}. Here, we mainly found inhibition of TCR signaling pathway in T cells. mTOR signaling was inhibited in CD4⁺ subsets but not in CD8⁺. This may explain the higher inhibitory effect of azithromycin on CD4⁺ compared to CD8⁺ cells. This also suggests that glycolysis inhibition may not uniquely be ascribed to mTOR pathway but also to upstream TCR signaling.

Single-cell analysis of gene expression revealed downregulation of mitochondrial genes after azithromycin exposure that was associated with impaired respiratory chain functions. Mitochondria metabolism produces ATP through oxidative phosphorylation and metabolites involved in the TCA and fatty acid oxidation⁴⁰. Others have already reported that blocking mitochondrial protein translation either leads to decreased cytotoxic and effector functions in T cells^{44,45}. Since azithromycin is known to inhibit bacterial ribosomal 50S subunit, azithromycin may thus also alter transcription of proteins involved in anti-tumor response such as IFN or TRAIL²³. We identified *SOCS1* as the most significantly upregulated gene, with higher protein expression after azithromycin exposure. SOCS1 was recently shown to abrogate Th1 responses, notably IFN- α and IL-2 synthesis³⁰. In a mice model, SOCS1 was shown to inhibit glycolysis through STAT3/HIF1a pathway⁴⁶. This mechanism may also explain glycolysis inhibition observed in T cells treated with azithromycin.

To conclude, studying samples from patients included in ALLOZITHRO trial allowed us to decipher how azithromycin promotes relapse. There is currently extensive literature

suggesting that antibiotics impact alloreactivity, illustrated by GvHD-related mortality through gut microbiota changes⁴⁷. Our results highlight that azithromycin directly affects immune cells and that these biological changes are associated with relapse after allo-HSCT. Knowing that GvHD incidence was not modified by azithromycin intake in the trial, the features identified in our study (and in others) including: Th2⁴⁸ and exhausted cells^{17,32,33}, or metabolically unfit T cells⁴¹ may be more broadly associated with post-transplant relapses mechanisms. Beyond the context of allo-HSCT, azithromycin is widely used in chronic respiratory diseases²³. Our results raise the question of the safety of using this treatment in patients at risk of cancer, such as chronic obstructive pulmonary disease patients⁴⁹.

Acknowledgments:

The authors thank all members of the CRYOSTEM Consortium and of the Francophone Society of Marrow Transplantations and Cellular Therapy (SFGM-TC) for providing patients samples used in this study and for their support. Authors thank Dr Marie-Hélène Schlageter, Dr Alessandro Donada and Dr Leila Perié (INSERM UMR168) for providing access to multiplex immunoassays instruments. Authors thank Dr Michaël Saitakis and Sebastian Amigorena (INSERM U932) for providing the CAR sequence. This work benefited from equipment and services from IGenSeq core facility, at ICM.

Author contributions:

Conceptualization: AB, DM; Methodology: DM, NV; Formal analysis: NV, SLG; Figures generation: NV, SLG, DM; Investigation: NV, SLG, LB, AC, BH, DB, LD, AB, MT, DG, EM, RI, KP, BI, PL; Resource: NV, AC, ST, PL, RPL, DM; Data Curation: NV, LB; Writing - Original Draft: NV, DM; Writing - Review and Editing: GS, AB, DM; Visualization: NV, DM; Supervision: DM; Project Administration: AB, DM; Funding Acquisition: GS, AB, DM

Funding:

This work was funded by the Association Leucémie Espoir, SOS oxygène, La Laurène, EGMOS association, HTC Project. NV was supported by the association Cancerologie du Centre and research grant from ITMO Cancer of Aviesan on funds administered by Inserm (ASC20047HSA). SLG was supported by La Fédération pour la Recherche Médicale and Association Capucine (M2R202106013386).

Competing interests: G.S. and R.P.L received a research grant from Alexion Pharmaceutical Company. R.P.L received a research grant from Novartis and Pfizer companies. G.S received 1457890 fees from Pharmacyclics LLC, Novartis, Incyte, Alexion, Amgen and Pfizer companies. D.M received fees from Novartis, Incyte, Jazz Pharmaceuticals and CSL Behring companies. All other authors have no conflict of interests to declare.

REFERENCES

1. Zeiser R, von Bubnoff N, Butler J, et al. Ruxolitinib for Glucocorticoid-Refractory Acute Graft-versus-Host Disease. *N Engl J Med.* 2020;382(19):1800–1810.
2. Zeiser R, Polverelli N, Ram R, et al. Ruxolitinib for Glucocorticoid-Refractory Chronic Graft-versus-Host Disease. *N Engl J Med.* 2021;385(3):228–238.
3. Zeiser R, Blazar BR. Acute Graft-versus-Host Disease — Biologic Process, Prevention, and Therapy. *N Engl J Med.* 2017;377(22):2167–2179.
4. Zeiser R, Blazar BR. Pathophysiology of Chronic Graft-versus-Host Disease and Therapeutic Targets. *N Engl J Med.* 2017;377(26):2565–2579.
5. Williams KM. Bronchiolitis Obliterans After Allogeneic Hematopoietic Stem Cell Transplantation. *JAMA.* 2009;302(3):306.
6. Bergeron A, Godet C, Chevret S, et al. Bronchiolitis obliterans syndrome after allogeneic hematopoietic SCT: phenotypes and prognosis. *Bone Marrow Transplant.* 2013;48(6):819–824.
7. Bergeron A, Chevret S, Peffault de Latour R, et al. Noninfectious lung complications after allogeneic hematopoietic stem cell transplantation. *Eur Respir J.* 2018;51(5):1702617.
8. Vos R, Vanaudenaerde BM, Verleden SE, et al. A randomised controlled trial of azithromycin to prevent chronic rejection after lung transplantation. *European Respiratory Journal.* 2011;37(1):164–172.
9. Bergeron A, Chevret S, Granata A, et al. Effect of Azithromycin on Airflow Decline-Free Survival After Allogeneic Hematopoietic Stem Cell Transplant: The ALLOZITHRO Randomized Clinical Trial. *JAMA.* 2017;318(6):557.
10. U.S. Food and Drug Administration. FDA warns about increased risk of cancer relapse with long-term use of azithromycin (Zithromax, Zmax) antibiotic after donor stem cell transplant. 2018;
11. Cheng G-S, Bondeelle L, Gooley T, et al. Azithromycin use and increased cancer risk among patients with bronchiolitis obliterans after hematopoietic cell transplantation. *Biology of Blood and Marrow Transplantation.* 2020;26(2):392–400.
12. Copelan EA. Hematopoietic Stem-Cell Transplantation. *New England Journal of Medicine.* 2006;(354):1813–1826.
13. Horowitz M, Schreiber H, Elder A, et al. Epidemiology and biology of relapse after stem cell transplantation. *Bone Marrow Transplant.* 2018;53(11):1379–1389.
14. Christopher MJ, Petti AA, Rettig MP, et al. Immune Escape of Relapsed AML Cells after Allogeneic Transplantation. *N Engl J Med.* 2018;379(24):2330–2341.
15. Toffalori C, Zito L, Gambacorta V, et al. Immune signature drives leukemia escape and relapse after hematopoietic cell transplantation. *Nat Med.* 2019;25(4):603–611.
16. Gambacorta V, Beretta S, Ciccimarra M, et al. Integrated Multiomic Profiling Identifies the Epigenetic Regulator PRC2 as a Therapeutic Target to Counteract Leukemia Immune Escape and Relapse. *Cancer Discovery.* 2022;candisc.0980.2021.
17. Noviello M, Manfredi F, Ruggiero E, et al. Bone marrow central memory and memory stem T-cell exhaustion in AML patients relapsing after HSCT. *Nat Commun.* 2019;10(1):1065.

18. Deng Q, Han G, Puebla-Osorio N, et al. Characteristics of anti-CD19 CAR T cell infusion products associated with efficacy and toxicity in patients with large B cell lymphomas. *Nat Med.* 2020;26(12):1878–1887.
19. Doan T, Hinterwirth A, Worden L, et al. Gut microbiome alteration in MORDOR I: a community-randomized trial of mass azithromycin distribution. *Nat Med.* 2019;25(9):1370–1376.
20. Zmora N, Bashiardes S, Levy M, Elinav E. The Role of the Immune System in Metabolic Health and Disease. *Cell Metabolism.* 2017;25(3):506–521.
21. CRYOSTEM. CRYOSTEM Biological Resources. *CRYOSTEM Biological Resources.* 2021;
22. Van Gassen S, Callebaut B, Van Helden MJ, et al. FlowSOM: Using self-organizing maps for visualization and interpretation of cytometry data: FlowSOM. *Cytometry.* 2015;87(7):636–645.
23. Parnham MJ, Haber VE, Giamarellos-Bourboulis EJ, et al. Azithromycin: Mechanisms of action and their relevance for clinical applications. *Pharmacology & Therapeutics.* 2014;143(2):225–245.
24. Koh A, Molinaro A, Ståhlman M, et al. Microbially Produced Imidazole Propionate Impairs Insulin Signaling through mTORC1. *Cell.* 2018;175(4):947-961.e17.
25. McDonald T, Puchowicz M, Borges K. Impairments in Oxidative Glucose Metabolism in Epilepsy and Metabolic Treatments Thereof. *Front. Cell. Neurosci.* 2018;12:274.
26. St. Paul M, Saibil SD, Han S, et al. Coenzyme A fuels T cell anti-tumor immunity. *Cell Metabolism.* 2021;33(12):2415-2427.e6.
27. Zhang Y-M, Chohnan S, Virga KG, et al. Chemical Knockout of Pantothenate Kinase Reveals the Metabolic and Genetic Program Responsible for Hepatic Coenzyme A Homeostasis. *Chemistry & Biology.* 2007;14(3):291–302.
28. Michonneau D. Metabolomics analysis of human acute graft-versus-host disease reveals changes in host and microbiota-derived metabolites. 2019;10(1):5695.
29. Pearce EL, Poffenberger MC, Chang C-H, Jones RG. Fueling Immunity: Insights into Metabolism and Lymphocyte Function. *Science.* 2013;342(6155):1242454.
30. Sutra Del Galy A, Menegatti S, Fuentealba J, et al. In vivo genome-wide CRISPR screens identify SOCS1 as intrinsic checkpoint of CD4+ TH1 cell response. *Sci Immunol.* 2021;6(66):eabe8219.
31. Scott AC, Dündar F, Zumbo P, et al. TOX is a critical regulator of tumour-specific T cell differentiation. *Nature.* 2019;571(7764):270–274.
32. Hutten TJA, Norde WJ, Woestenenk R, et al. Increased Coexpression of PD-1, TIGIT, and KLRG-1 on Tumor-Reactive CD8+ T Cells During Relapse after Allogeneic Stem Cell Transplantation. *Biology of Blood and Marrow Transplantation.* 2018;24(4):666–677.
33. Gournay V, Vallet N, Peux V, et al. Immune landscape after allo-HSCT: TIGIT and CD161-expressing CD4 T cells are associated with subsequent leukemia relapse. *Blood.* 2022;blood.2022015522.

34. Helmink BA, Reddy SM, Gao J, et al. B cells and tertiary lymphoid structures promote immunotherapy response. *Nature*. 2020;577(7791):549–555.
35. Magenau JM, Peltier D, Riwes M, et al. Type 1 interferon to prevent leukemia relapse after allogeneic transplantation. *Blood Advances*. 2021;5(23):5047–5056.
36. Shankaran V, Ikeda H, Bruce AT, et al. IFN γ and lymphocytes prevent primary tumour development and shape tumour immunogenicity. *Nature*. 2001;410(6832):1107–1111.
37. Walczak H, Miller RE, Ariail K, et al. Tumoricidal activity of tumor necrosis factor-related apoptosis-inducing ligand in vivo. *Nat Med*. 1999;5(2):157–163.
38. Wynn TA. Type 2 cytokines: mechanisms and therapeutic strategies. *Nat Rev Immunol*. 2015;15(5):271–282.
39. Martins CP, New LA, O'Connor EC, et al. Glycolysis Inhibition Induces Functional and Metabolic Exhaustion of CD4+ T Cells in Type 1 Diabetes. *Front. Immunol*. 2021;12:669456.
40. Chapman NM, Chi H. Metabolic adaptation of lymphocytes in immunity and disease. *Immunity*. 2022;55(1):14–30.
41. Uhl FM, Chen S, O'Sullivan D, et al. Metabolic reprogramming of donor T cells enhances graft-versus-leukemia effects in mice and humans. *Sci. Transl. Med*. 2020;12(567):eabb8969.
42. Finlay DK, Rosenzweig E, Sinclair LV, et al. PDK1 regulation of mTOR and hypoxia-inducible factor 1 integrate metabolism and migration of CD8+ T cells. *Journal of Experimental Medicine*. 2012;209(13):2441–2453.
43. Salmond RJ. mTOR Regulation of Glycolytic Metabolism in T Cells. *Front. Cell Dev. Biol*. 2018;6:122.
44. Lisci M, Barton PR, Randzavola LO, et al. Mitochondrial translation is required for sustained killing by cytotoxic T cells. *Science*. 2021;374(6565):eabe9977.
45. Almeida L, Dhillon-LaBrooy A, Castro CN, et al. Ribosome-Targeting Antibiotics Impair T Cell Effector Function and Ameliorate Autoimmunity by Blocking Mitochondrial Protein Synthesis. *Immunity*. 2021;54(1):68–83.e6.
46. Piñeros Alvarez AR, Glosson-Byers N, Brandt S, et al. SOCS1 is a negative regulator of metabolic reprogramming during sepsis. *JCI Insight*. 2017;2(13):e92530.
47. Shono Y, Docampo MD, Peled JU, et al. Increased GVHD-related mortality with broad-spectrum antibiotic use after allogeneic hematopoietic stem cell transplantation in human patients and mice. *Science Translational Medicine*. 2016;8(339):16.
48. Jung U, Foley JE, Erdmann AA, Eckhaus MA, Fowler DH. CD3/CD28-costimulated T1 and T2 subsets: differential in vivo allosensitization generates distinct GVT and GVHD effects. *Blood*. 2003;102(9):3439–3446.
49. de Torres JP, Marín JM, Casanova C, et al. Lung Cancer in Patients with Chronic Obstructive Pulmonary Disease: Incidence and Predicting Factors. *Am J Respir Crit Care Med*. 2011;184(8):913–919.

FIGURE LEGENDS

Figure 1. Overview of the samples studied according to omics assays. Frozen peripheral mononuclear blood cells, plasma and cell pellets from patients included in the double blinded ALLOZITHRO study were retrieved from national CRYOSTEM biobank. All samples were collected after allogeneic hematopoietic stem cell transplantation, either at time of acute graft versus host disease or at the nearest visit by day 100. Patients' characteristics and outcome are depicted in **Supplemental Table S1** and **Supplemental Figure S2**.

Figure 2. Azithromycin intake is associated with immune cells subsets changes. **(A)** Frozen peripheral mononuclear blood cells (PBMC) from patients included in placebo (PLA, n=106) or azithromycin (AZM, n=98) arm and from healthy donors (n=20) were thawed and analyzed by mass cytometry with a panel targeting 43 antigens used to cluster cells according to their phenotype and T cells functional state (naïve, activated or exhausted). Pre-processing pipeline was used to normalize data across batches and then identify singlets, CD45+ living cells. Fifty-five cells phenotypical subsets were identified by using 31 phenotype antigens with FlowSOM algorithm. **(B)** Circular dendrogram showing the 55 cells subsets hierarchy colored according to the corresponding subsets and sized by frequency among CD45+ cells. **(C)** Uniform manifold approximation and projection (UMAP) depicting cells clustering colored according to their subsets. **(D)** Boxplots representing percentage of main PBMC subsets among living CD45+ according to sample groups. **(E)** Heatmap representing scaled expression of phenotypes antigen across the cell subsets manually ordered and annotated for visualization purposes. Targeted antigens are ordered by hierarchical clustering and unidentified cell subsets are shown in

Supplemental Figure S4. Fold changes of immune subsets in AZM group compared to PLA group are summarized with a bar plot (* $p<0.05$; ** $p<0.01$, P values are shown in f panel). Bold names of subsets indicate significant difference. **(F)** Boxplots of statistically different subsets between AZM and PLA cohorts. For visualization purposes, square root transformation was applied on y-axis. All P values were calculated with two-sided Wilcoxon signed rank test. NK: natural killer, DN: double negative, EM: effector memory, EMRA: effector memory CD45RA+, Non-conv: non-conventional, MAIT: mucosal associated invariant T cells.

Figure 3. T cells exhausted profiles are observed in patients treated with azithromycin. (A) Heatmap representing scaled expression of 14 functional antigens used to identify 25 functional state clusters with FlowSOM algorithm among 30 T cells phenotypical subsets. Below, a dot plot shows percentage of functional state clusters in each T cells subsets. Functional state clusters with only more than four percent of the corresponding cell subsets are drawn. Letters indicates a significant difference between azithromycin and placebo groups and the corresponding panel. **(B-F)** Boxplots of statistically different states subsets between azithromycin and placebo cohorts. For visualization purposes, square root transformation was applied on y-axis. All P values were calculated with two-sided Wilcoxon signed rank test.

Figure 4. Azithromycin treatment and relapse are associated with changes in cell energy metabolism pathways. (A-B) Metabolomic analyses in plasma **(A)** and dried cell pellets **(B)** samples. Volcano plots and dot plots illustrate metabolites individual changes and pathway enrichment in patients treated by azithromycin (AZM) are compared to placebo (PLA). Volcano plots P values were calculated with two-sided Wilcoxon signed rank test; enrichment P values

were computed with hypergeometric test. **(C)** Omics integration method overview. Ninety-eight and 87 patients with mass cytometry, plasma and cell metabolomics samples in PLA and AZM cohorts were studied, respectively. Variables identified as statistically different between the two groups were used to reduce dimensionality with principal component analysis (PCA). Number of components to study was defined by a threshold of 80% cumulative percentage of variance explained. Patients coordinates in a 29 dimensions space were extracted from PCA result. **(D)** Forest plot representing the hazard ratio of relapse with the corresponding 95% confidence interval of a multivariate Fine-Gray model including each component and treatment groups as covariates with death as the competing event. Blue dots indicate principal components statistically associated with relapse. **(E)** Stacked bar plot depicting percentage of contribution of variables from each omics layers in the three components associated with relapse. Top contributing individual variables are shown in Extended Data Figure 1. **(F)** Chord diagram showing statistically significant inter-omic correlations. **(G)** Correlation networks of variables included in the multi-omics analyses. Nodes coordinates were calculated with multidimensional scaling algorithm and edges are drawn between correlated variables. Variable (node) that significantly contributed to relapse are illustrated by the blue color and size is correlated to the corresponding sum of contribution in significant dimensions. Area where nodes overlaid are zoomed and highlighted in yellow for visualization purposes. P value and correlation and coefficients were computed according to Spearman's rank correlation. Correlations were considered statistically significant if adjusted P values with false discovery rate were below 0.05 and Spearman's absolute rho value above 0.3.

Figure 5. Azithromycin treatment is associated with enrichment of energy metabolism, cell cycle and immune response pathways. (A) Frozen peripheral mononuclear blood cells (PBMC) from patients (placebo, n=14 and azithromycin, n=17) were thawed and analyzed by cellular indexing of transcriptomes and epitopes by sequencing (CITE-Seq). Cells were clustered according to cell surface antigen expression. (B) Uniform manifold approximation and projection (UMAP) describing cells clustering. (C) Heatmap depicting scaled cell surface antigen expression in cell subsets. (D) Dot plot depicting enrichment analysis within each subset of cells using Hallmark gene sets. Only immune cells with at least one enriched pathway are depicted. P values were computed with adaptive multi-level split Monte-Carlo and adjusted with false discovery rate. (E) Cell cycle analysis from CITE-Seq with cell cycle score. P values were computed with two-sided matched-pair Wilcoxon rank test. NK: natural killer, DN: double negative, EM: effector memory, EMRA: effector memory CD45RA+, MAIT: mucosal associated invariant T cells, Clas.: classical, Int.: intermediate.

Figure 6. Azithromycin inhibits T cells proliferative and cytotoxic functions by impeding energetic boost from glycolysis. (A) Sorted CD3+ cells from healthy donors (HD) peripheral mononuclear blood cells (PBMC) were stained with carboxyfluorescein succinimidyl ester (CFSE) and treated in vitro with azithromycin (AZM) or control (CTRL) for 24 hours before activation with anti-CD3/CD28 beads. Two days after activation, cells were retrieved from incubator and analyzed by flow cytometry. CFSE staining in CD4+ and CD8+ T cells subsets are shown in histograms (representative results) and boxplots (each dot is the median value of 3 technical replicates). Results are from three independent experiments with six independent HD. (B) Anti-CD19 chimeric antigenic receptor (CAR)-T cells were cultured with AZM or control

for 24 hours and co-cultured with luciferase expressing CD19+ NALM6 cell lines overnight. Cell lysis was quantified by luminescence. Representative result is shown as a dot plot and pooled six independent experiments are depicted in boxplots. **(C)** Cell energy metabolism overview and corresponding glycolysis and oxidative phosphorylation (OXPHOS) assays from HD sorted CD4+ and CD8+ cells after 24 hours of incubation with AZM or DMSO (CTRL). Extracellular acidification rate (ECAR) and oxygen consumption rate (OCR) were measured at time of activation with anti-CD3/CD28 antibody complexes then glycolysis was inhibited with 2-deoxyglucose (2-DG). Dot plots show representative results and boxplots pooled results from 6 independent experiments. All P values were computed with two-sided matched-pair Wilcoxon rank test.

Figure 7. Azithromycin inhibits TCR signaling in T cells, promotes immunomodulatory pathways and impedes mitochondrial mRNA synthesis. (A) Thawed PBMC from eight healthy donors (HD) were treated with azithromycin (AZM) or control (CTRL) for 24 hours before CD3/CD28 activation. Activation was stopped at 0, 3, 5, 10 and 30 minutes. To prevent batch effect on sample labelling, samples from each donor were barcoded with a mix of anti-CD45 antibodies then pooled before mass cytometry staining procedure. Single cells were then clustered with FlowSOM algorithm according to phenotype antigens expression. Area under the curve (AUC) of signaling mean signal intensity was computed. Clusters' phenotypes are available in **Supplemental Figure S18**. **(B)** Dot plot depicting statistically significant difference in AUC between CTRL and AZM conditions. Individual differences at the 5 time-points are available in **Supplemental Figure S20**. P values were computed with matched-paired Wilcoxon Rank Sum test. pSTAT6 is not depicted as it was not statistically different. **(C)** CD3+ sorted

cells from ten HD were treated with AZM or CTRL for 24 hours before CD3/CD28 activation. Analysis was performed two days 2 following cells activation. Pie chart illustrating the number of living cells retrieved at the end of the single cell RNA sequencing with cell surface antigen embedding pipeline. Next, using cell surface antigen expression, 26 phenotypical cell clusters were identified as illustrated with the Uniform manifold approximation and projection (UMAP).

(D) UMAP highlighting retrieved cells from activated conditions. (E) Heatmap representing manually ordered and annotated cell clusters with the corresponding scaled surface antigen expression. Abundances of clusters in cells treated with AZM or CTRL are depicted on boxplots. For visualization purposes, square root transformation was applied on x-axis. P values were computed with matched-paired Wilcoxon Rank Sum test. (F) Dot plot showing differentially expressed genes in each T cells clusters from volcano plots shown in **Supplemental Figure S21**. Only statistically significant changes are depicted. P values were computed with Wilcoxon Rank Sum test and adjusted with false discovery rate.

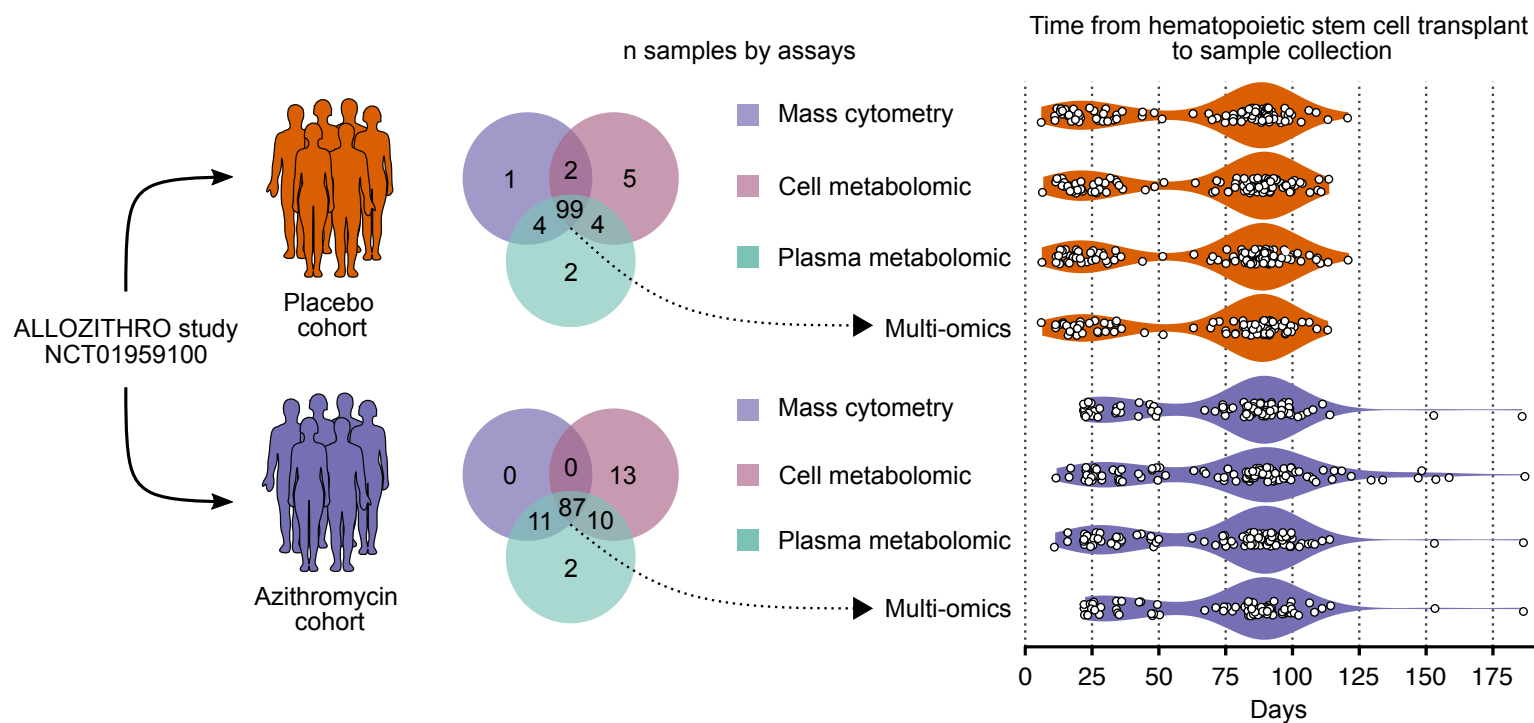


Figure 1

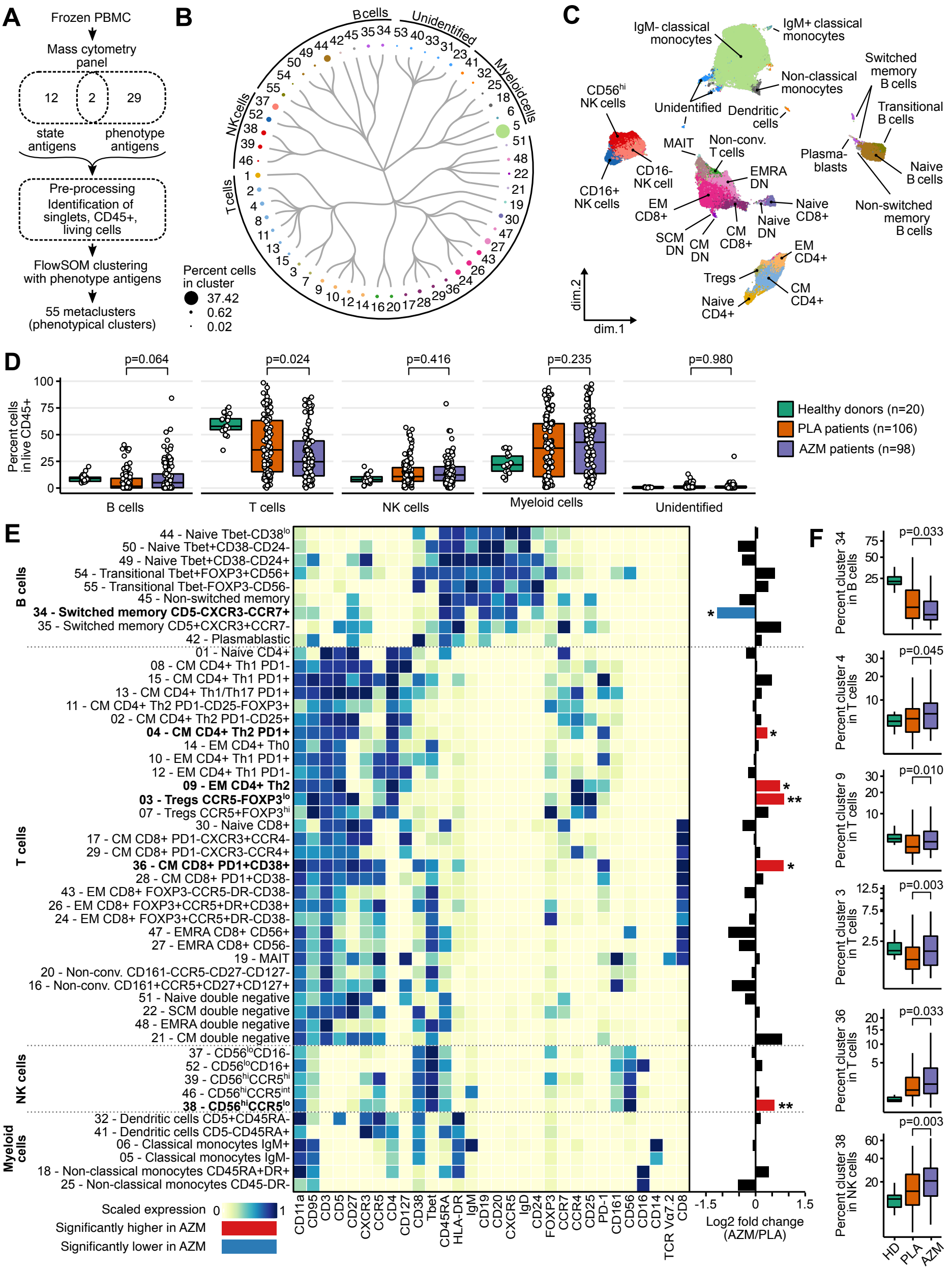
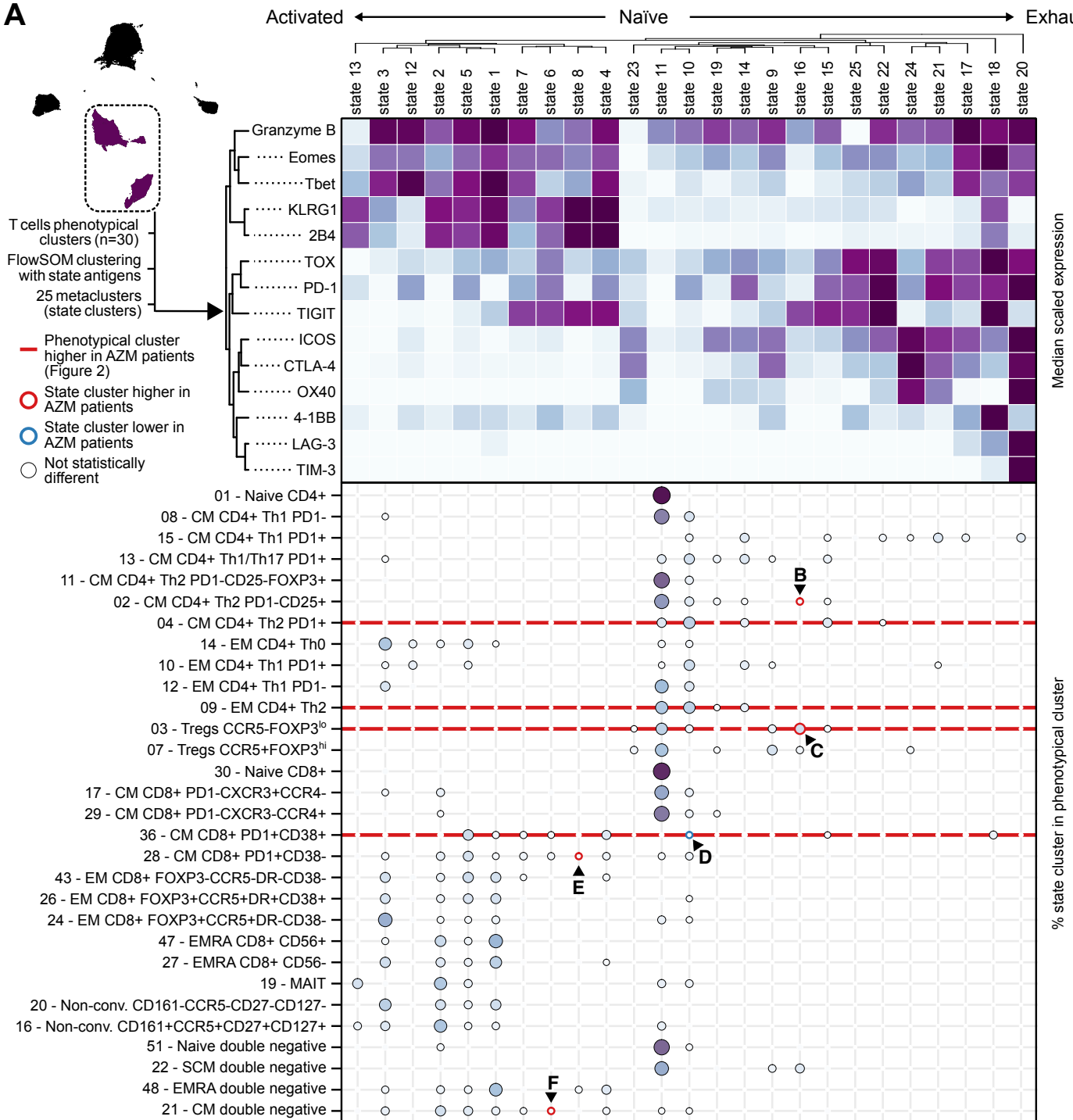
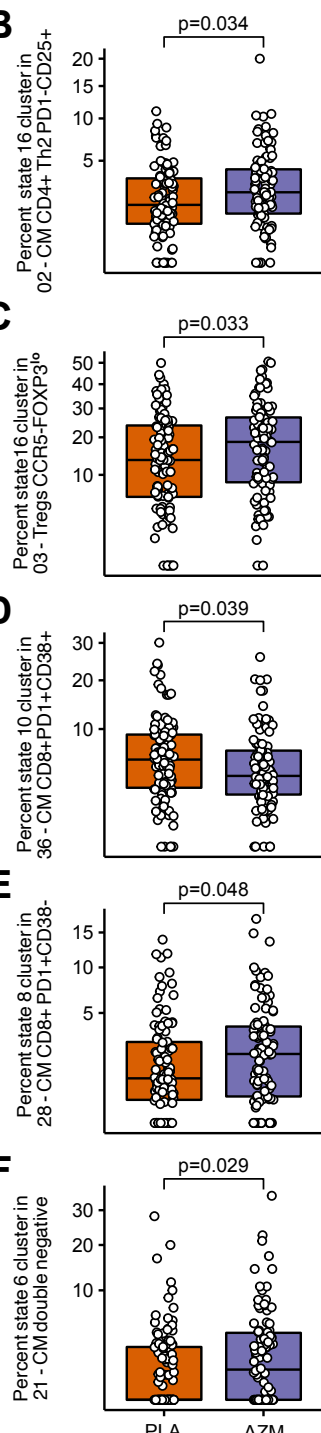


Figure 2

A**B****Figure 3**

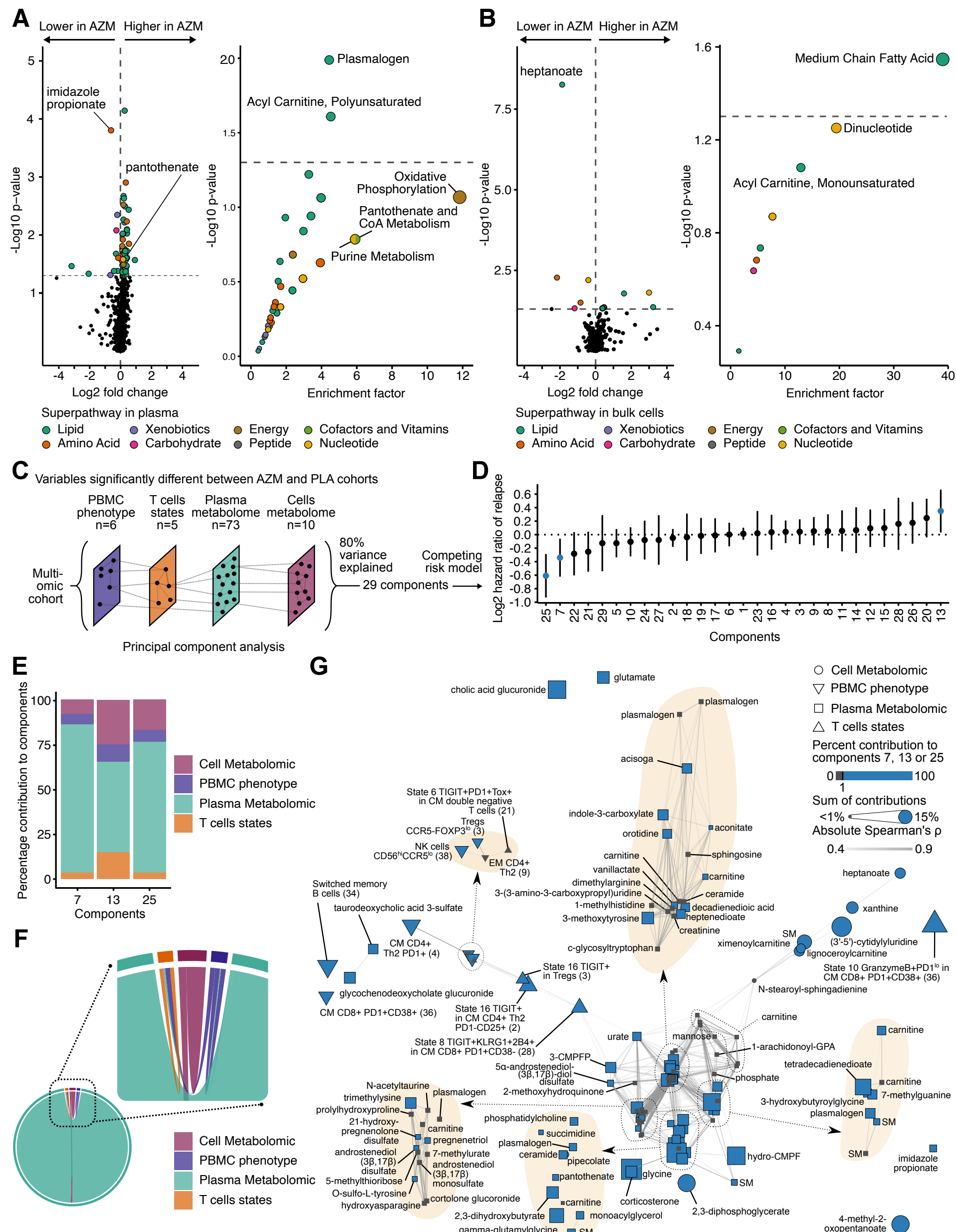


Figure 4

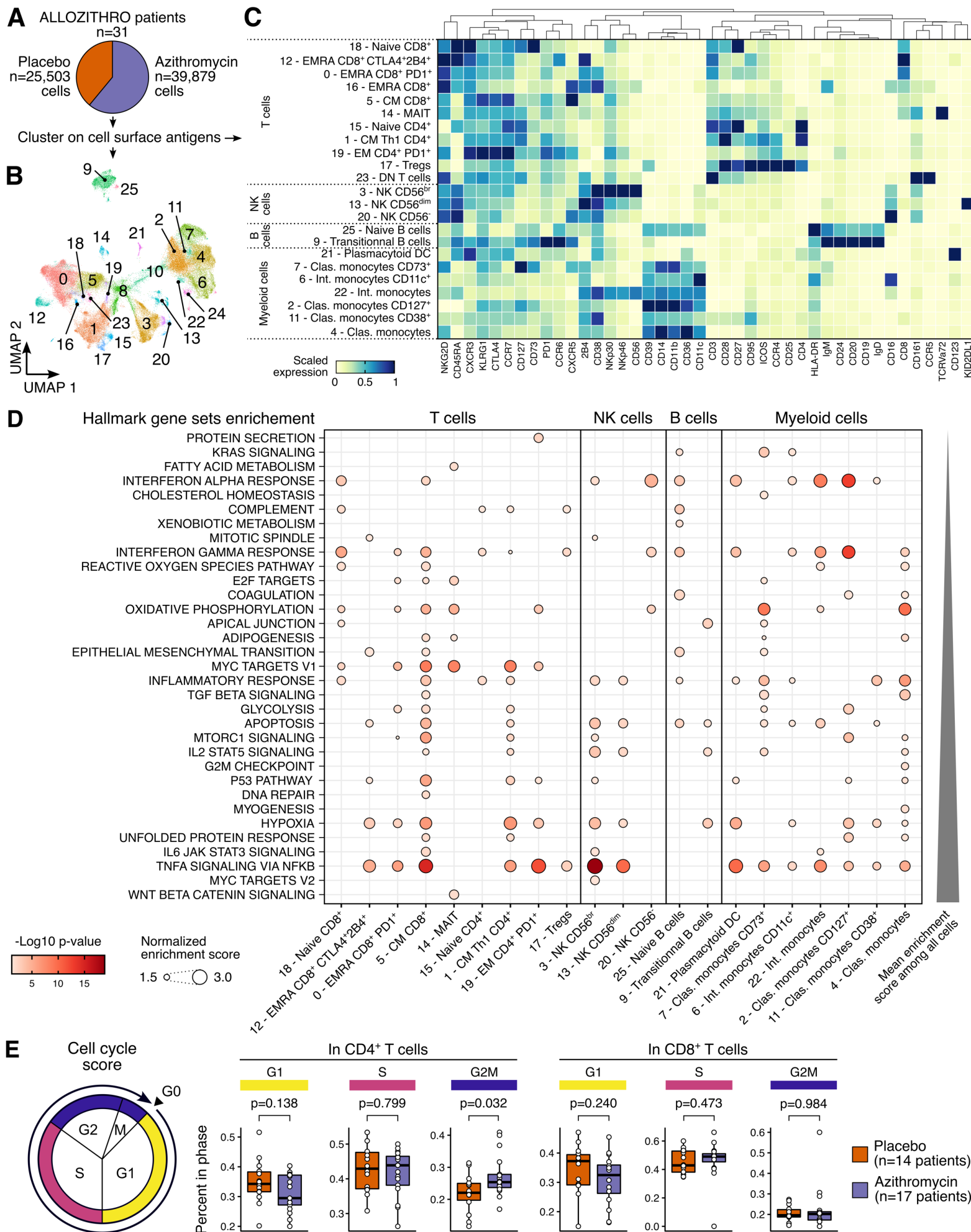
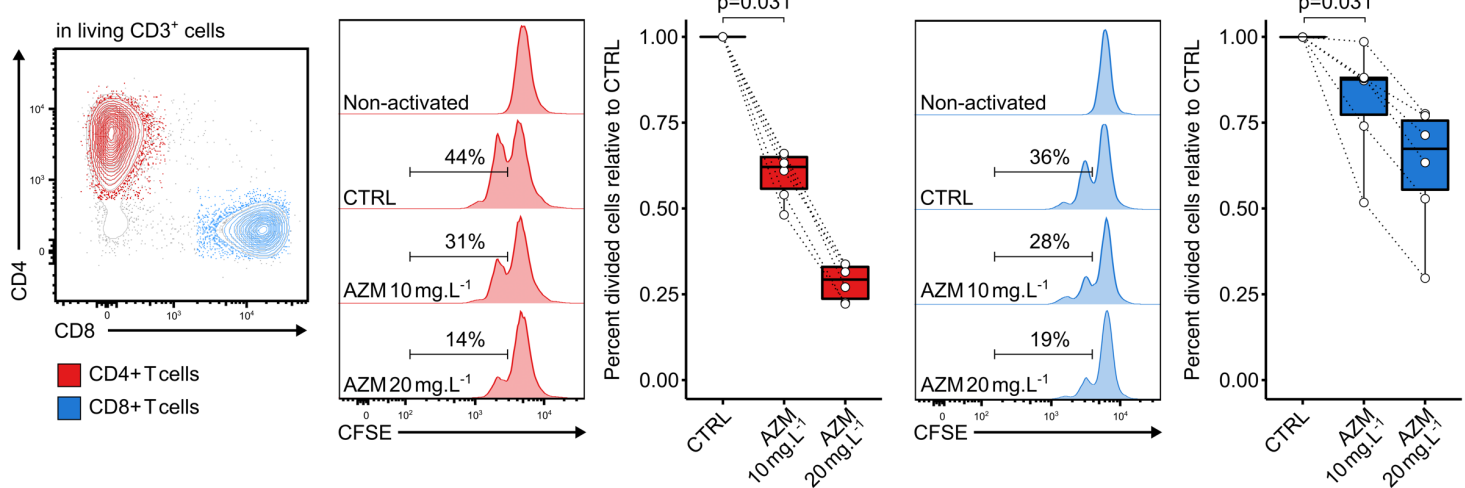
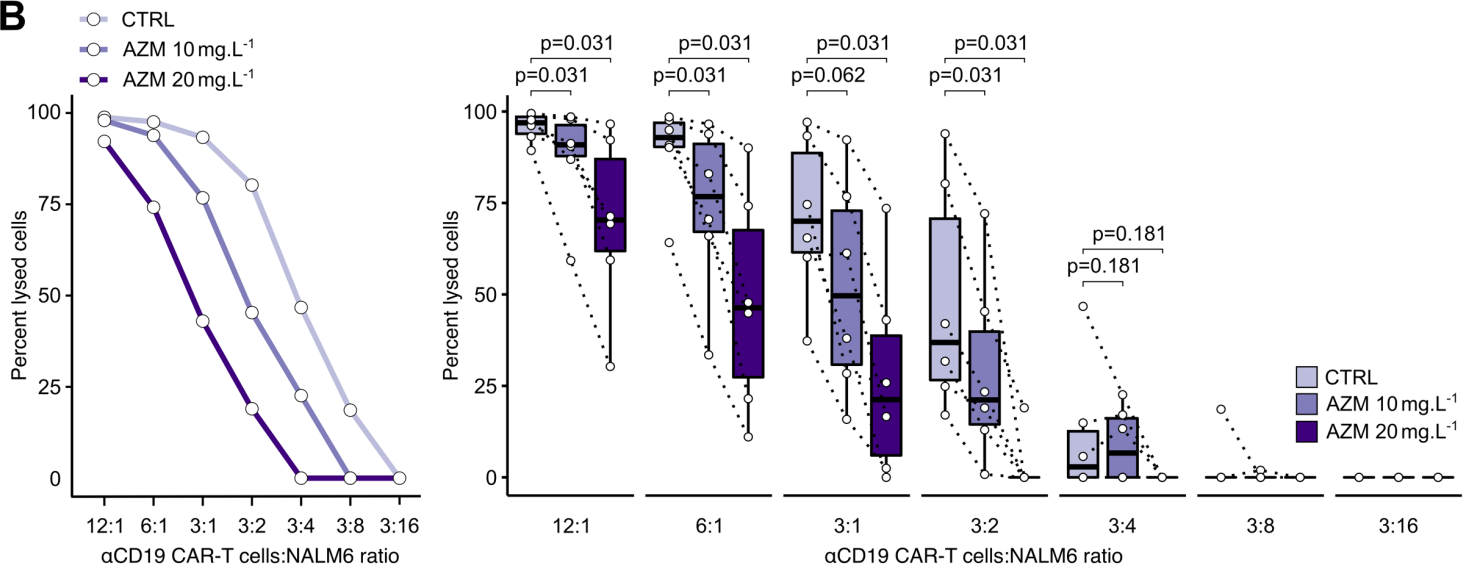
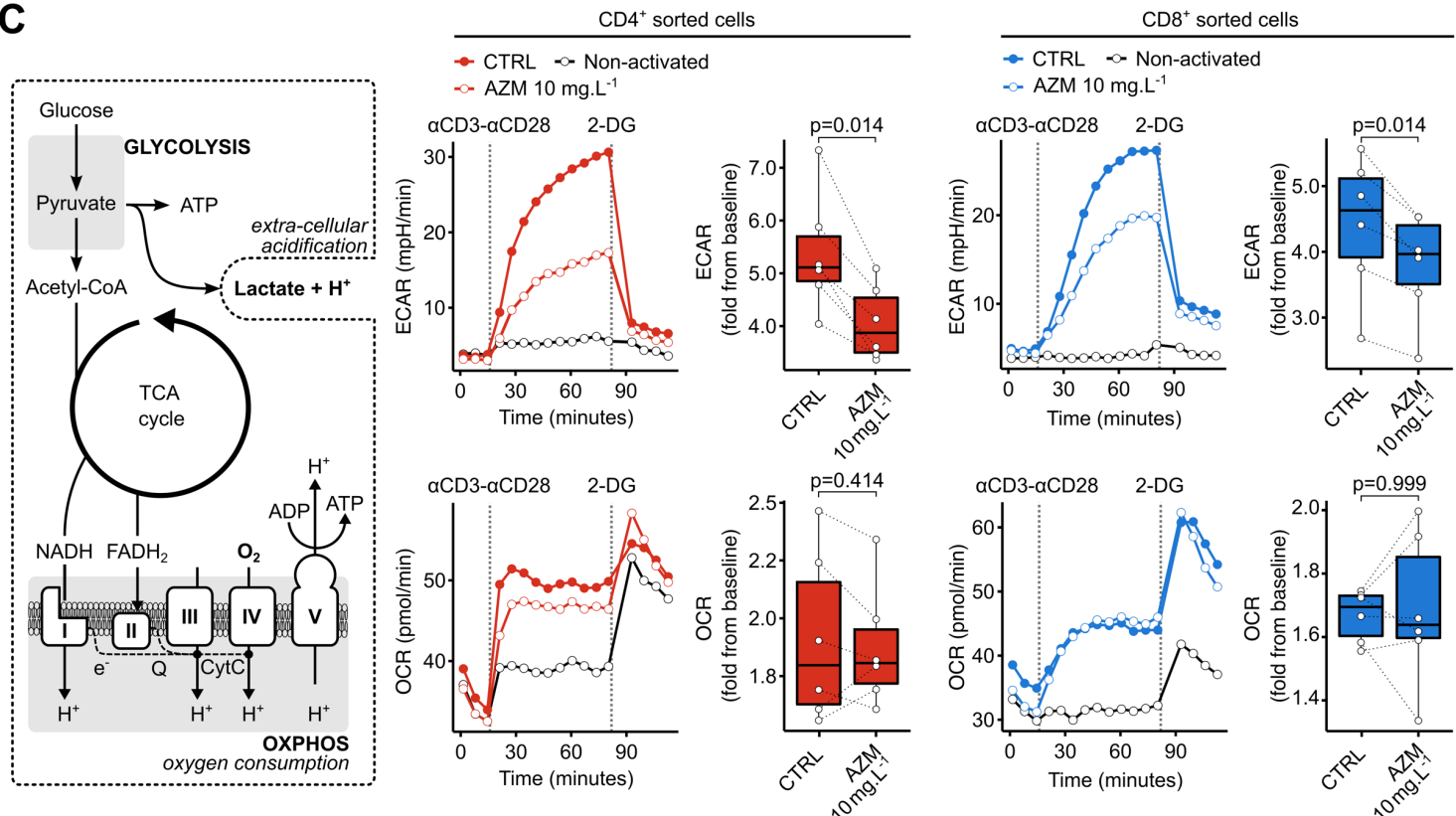


Figure 5

A**B****C****Figure 6**

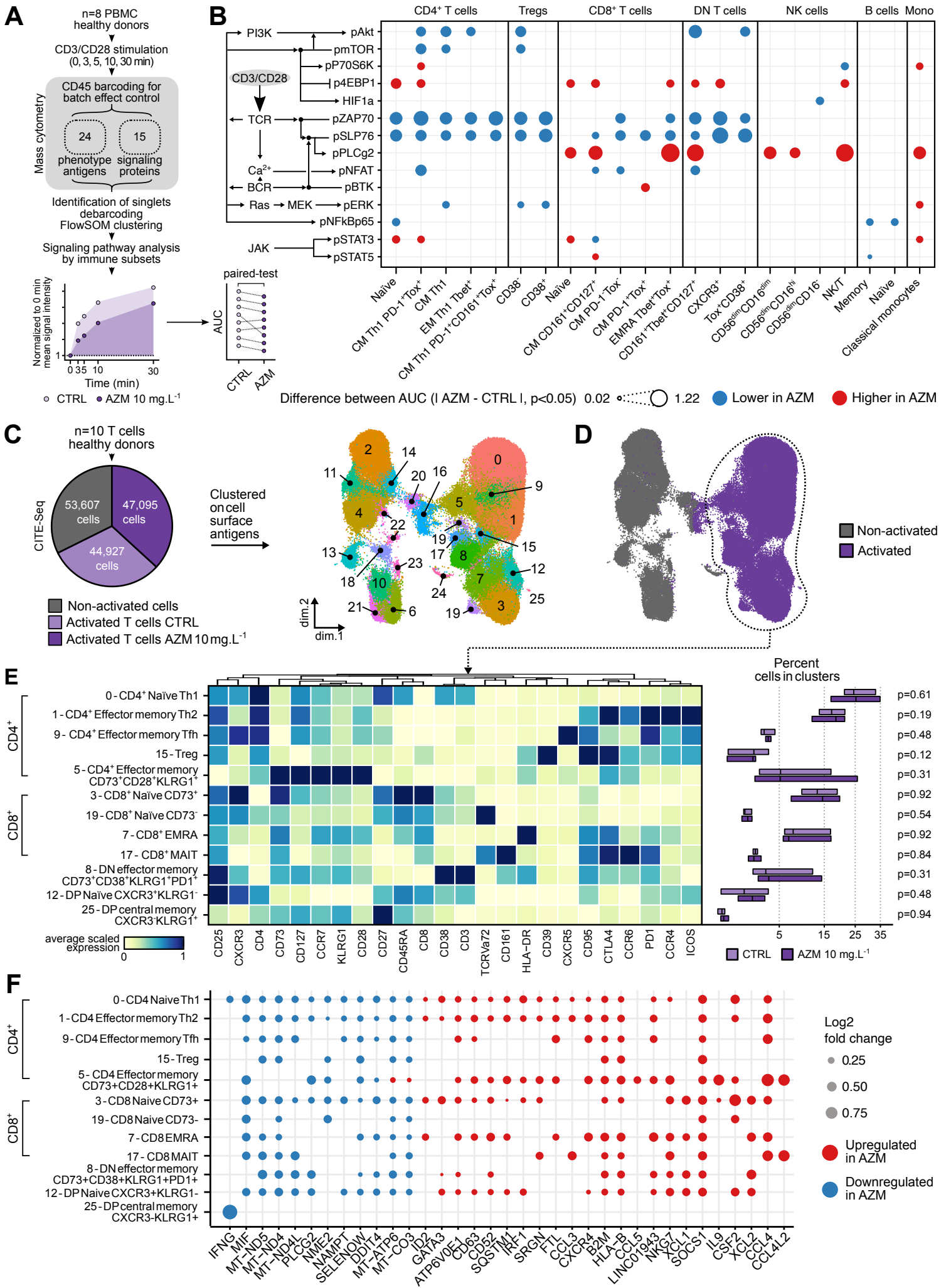


Figure 7